Studies of the β-sheet mediated self-assembly of designed synthetic peptides of general formula PhCO-Gly-Xx-OCH_2Ph and the possible role of aromatic π-π interactions in the self-assembly

Arpita Dutta,[a] Sudeshna Kar,[a] Roland Fröhlich,[b] Pradyot Koley,[a] and Animesh Pramanik*[a]

[a]*Department of Chemistry, University of Calcutta, 92, A. P. C. Road, Kolkata-700 009, India*
[b]*Organisch-Chemisches Institut, Universität Münster, Corrensstraße 40, D-48149, Münster, Germany*
E-mail: animesh_in2001@yahoo.co.in

Abstract

A set of three peptides **1-3** of general formula PhCO-Gly-Xx-OCH_2Ph, where Xx is Gly in peptide **1**, Ala in **2** and Aib (α-animo isobutyric acid) in **3** has been chosen to study the self-assembly and the morphology of the solid biomaterials. FT-IR and single crystal X-ray diffraction studies reveal that the peptides **1-3** self-assemble to form supramolecular β-sheet structures through intermolecular hydrogen bonds and aromatic π-π interactions. Field emission scanning electron micrographs (FE-SEM) of the dried materials of the peptides **1-3** show the formation of flat ribbon like structures which are formed through β-sheet mediated self-assembly.

Keywords: Peptides, self-assembly, supramolecular β-sheet, aromatic π-π interactions, ribbon-like structures

Introduction

Generally peptides are efficient building blocks for producing nanoscopic materials through self-assembly.[1, 2] Designed small peptides that self-assemble into β-sheet fibrils may find useful applications in tissue engineering and fabricating biomaterials.[3] Under suitable condition self-aggregating β-sheet forming peptides can create gels,[4] and provide molecular scaffolds for growing neurons and cartilage.[3a, 5] It has been established that β-sheet-driven aggregation of mis-folded proteins is responsible for various neurodegenerative diseases such as Alzheimer's disease,[6] Parkinson's disease,[7] and prion related diseases.[8] Therefore design and construction of β-sheets is important if a better understanding of the peptide self-aggregation mechanism to be gained.

It has been observed that aromatic π-π interactions play a crucial role in many areas of chemistry and biochemistry, most notably in molecular recognition and self-assembly.[9] Aromatic π-π interactions are known to provide energetic contribution as well as order and directionality in the self-assembly of amyloid structures.[10] Generally, short peptides with aromatic side chains are found to have the ability to form β-sheet mediated amyloid fibrils.[10, 11] In this context, we chose a set of three peptides **1-3** of general formula PhCO-Gly-Xx-OCH_2Ph where Xx is Gly in peptide **1**, Ala in **2** and Aib (α -animo isobutyric acid) in **3** to examine the role of aromatic π-π interactions in self-assembly (Fig. 1). The incorporation of Gly is expected to provide extended and semi-extended conformations in the back-bone of the peptides. The investigation would establish whether the peptides **1-3** produce the same supramolecular structure and morphologically similar materials through their self-assembly or differ significantly. Peptides **1-3** were synthesized using conventional solution phase methodology and their solid state structures were determined by FT-IR and X-ray diffraction analysis. The morphological features of the biomaterials generated from the peptides **1-3** in the solid state were examined by field emission scanning electron microscopy (FE-SEM).

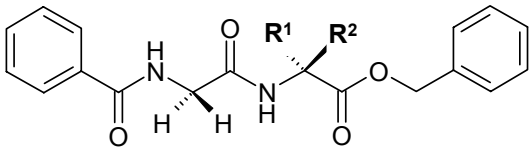

Peptide **1**: $R^1 = H$; $R^2 = H$
Peptide **2** : $R^1 = H$; $R^2 = CH_3$
Peptide **3** : $R^1 = CH_3$; $R^2 = CH_3$

Figure 1. Schematic representation of peptides **1-3**.

Results and Discussion

FT-IR study

The preliminary information about the peptide conformation was obtained from solid state FT-IR studies. In the solid state (KBr matrix) all the peptides **1-3** show intense bands at 3286-3368 cm^{-1} indicating the presence of strongly hydrogen bonded NH groups (Fig. 2). Important IR data for all the peptides are listed in Table 1. The absence of a band attributed to free NH (over 3430 cm^{-1}) indicates that all the NH groups in peptides **1-3** are involved in intermolecular hydrogen bonding. The CO stretching band at around 1647-1656 cm^{-1} (amide I), and the NH bending peak near 1530-1552 cm^{-1} (amide II) suggest the presence of intermolecular hydrogen bonded supramolecular β-sheet-like conformations for all the peptides in the solid state (Fig. 2).[12] The bands around 1736-1752 cm^{-1} are due to the CO stretching frequencies of free ester groups (-CO_2CH_2Ph). Therefore the solid-state FT-IR data supports the hypothesis that the

peptides adopt the β-sheet-like structures in the solid state. In order to obtain detailed information about the intermolecular hydrogen bonding networks, aromatic π-π interactions and self-assembly mechanisms, single crystal X-ray diffraction studies were carried out.

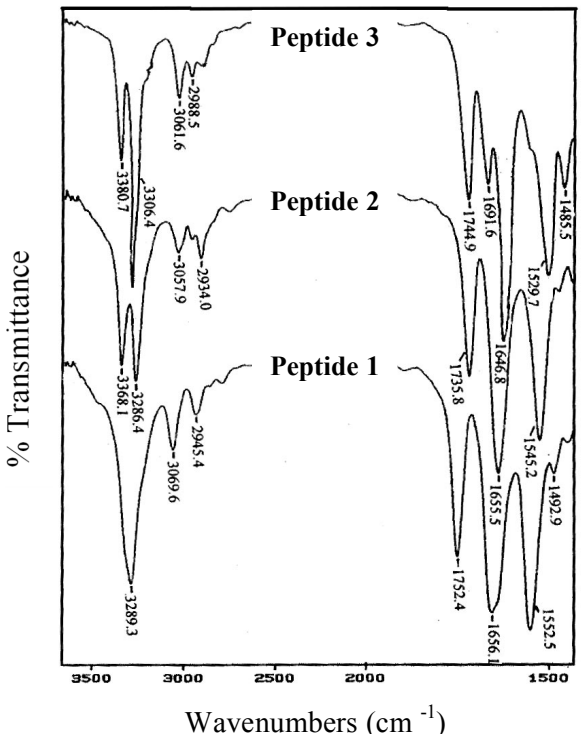

Figure 2. FT-IR spectra at the region 3200-3500 cm^{-1} (a) and 1500-1750 cm^{-1} (b) of peptides **1-3** in the solid state.

Table 1. Infrared (IR) absorption frequencies (cm^{-1}) for peptides **1-3** in solid state (KBr pellet)

Peptide	CO stretch	NH bend	NH stretch
Benz-Gly-Gly-OBz (**1**)	1752 (s), 1656 (s)	1552 (s)	3289 (s)
Benz-Gly-Ala-OBz (**2**)	1736 (s), 1655 (s)	1545 (m)	3368(s), 3286 (s)
Benz-Gly-Aib-OBz (**3**)	1745 (s), 1647 (s)	1530 (m)	3381 (w), 3306 (s)

s=strong, m=medium, w=weak.

Single crystal X-ray diffraction studies

The colourless orthorhombic crystals of peptide PhCO-Gly(1)-Gly(2)-OCH_2Ph (**1**) were obtained from a $CHCl_3$-petroleum ether mixture by slow evaporation. The molecule crystallizes in space group *P*bca with one molecule in the asymmetric unit. A diagram of peptide **1** is presented in Fig. 3. The backbone torsion angles (φ, *ψ*), that characterize the extended conformation, are φ_1 = -

80.8°, ψ_1 = 159.7° at Gly(1) and φ_2 = -72.0°, ψ_2 = 148.1° at Gly(2) (Table 2). The incorporation of Gly in the sequence helps to attain a fully extended conformation, which is necessary for β-sheet formation. In the solid state the molecules are connected via intermolecular hydrogen bond between Gly(1)-NH of one molecule with Ph-CO of another (N9---O8, 2.85 Å) along *c*-axis to create an infinite strand-like structure where the molecules are arranged in anti-parallel fashion (Fig. 4a, Table 3). Several such strand like structures are self-assembled in *b* direction to form two dimensional (*b*, *c* axis) layers of β-sheet through zipper-like assembly stabilized by van der Waals interactions between the phenyl rings (Fig. 4a). Again the molecules of **1** are packed in *a* direction through intermolecular hydrogen bond between Gly(2)-NH of one molecule with Gly(1)-CO of another (N13---O12, 2.83 Å) in parallel fashion (Fig. 4b, Table 3). The arrangement is further stabilized by aromatic π-π interactions between the two neighbouring phenyl rings of the benzoyl groups with an average distance of 4.57 Å between the eclipsed C atoms.[13] Therefore the β-sheet layers (*b*, *c* axis) of peptide **1** are stacked one on top of the other in *a* direction to form laminated supramolecular β-sheet assembly in the solid state.

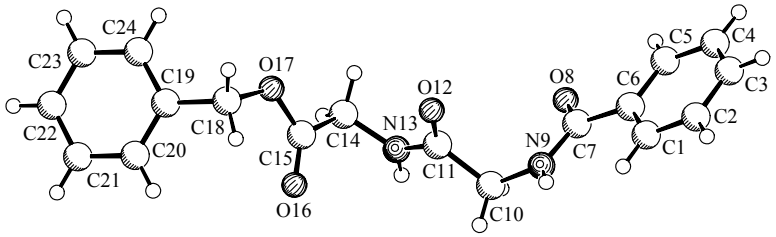

Figure 3. SCHAKAL diagram of peptide **1** with atom numbering scheme.

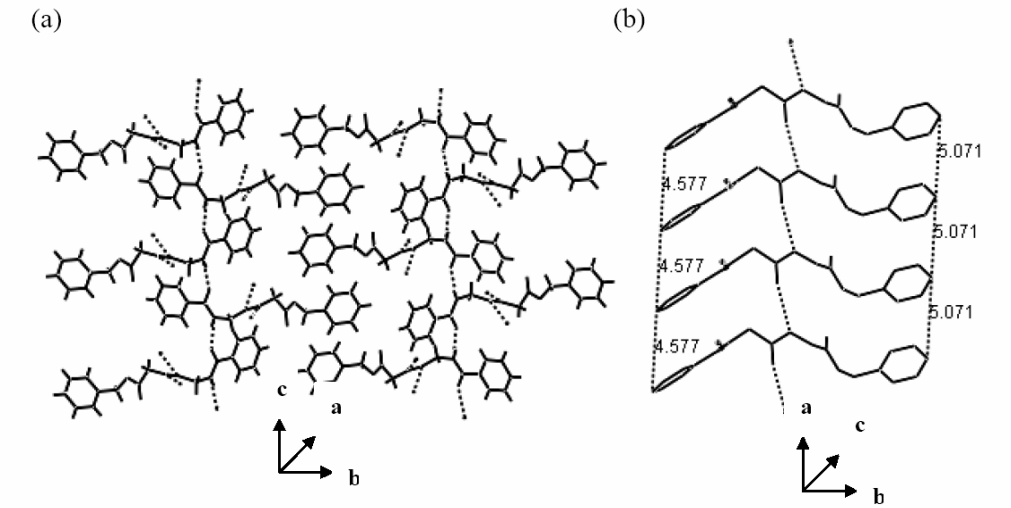

Figure 4. (a) Packing diagram of peptide **1** showing the formation of two dimensional (*b*, *c* axis) layer of β-sheet through zipper-like self-assembly driven by intermolecular hydrogen bond (between N9--08) and van der Waals interactions; (b) Packing of peptide **1** in *a* direction through intermolecular hydrogen bond (between N13---O12) and π-π interactions. Intermolecular hydrogen bonds are shown as dotted lines.

Table 2. Selected back-bone torsion angles (deg) for peptides **1-3**

Peptide **1**			
C6-C7-N9-C10 (ω_0)	-177.7(2)	C10-C11-N13-C14(ω_1)	177.6(2)
C7-N9-C10-C11 (φ_1)	-80.8(3)	C11-N13-C14-C15 (φ_2)	-72.0(3)
N9-C10-C11-N13 (ψ_1)	159.67(2)	N13-C14-C15-017 (ψ_2)	148.1(2)
Peptide **2**			
C6-C7-N9-C10 (ω_0)	177.1(2)	C10-C11-N13-C14(ω_1)	-174.5(2)
C7-N9-C10-C11 (φ_1)	-87.6(2)	C11-N13-C14-C16 (φ_2)	-154.9(2)
N9-C10-C11-N13 (ψ_1)	-166.5(2)	N13-C14-C16-018 (ψ_2)	-168.7(2)
Peptide **3**			
C6-C7-N9-C10(ω_0)	-178.7(2)	C10-C11-N13-C14 (ω_1)	-173.6(2)
C7-N9-C10-C11 (φ_1)	-168.6(2)	C11-N13-C14-C17 (φ_2)	54.0(2)
N9-C10-C11-N13 (ψ_1)	179.8(2)	N13-C14-C17-019 (ψ_2)	-155.2(2)

Table 3. Intermolecular hydrogen bonding parameters of peptides **1-3**

D-H---A	H---A/ Å	D---A/ Å	D-H---A/^{o}
Peptide **1**			
N9-H9---O8[a]	1.99	2.853	166.5
N13-H13---O12[b]	1.97	2.826	165.9
Peptide **2**			
N9-H9---O8[c]	2.06	2.860	151.1
N13-H13---O12[d]	2.07	2.903	164.9
Peptide **3**			
N13-H13---O8[e]	2.07	2.901	171.8

Symmetry equivalents: [a] x - 0.5, y, -z + 0.5; [b] – x +1.5, y + 0.5, z; [c] - x, y - 0.5, - z + 1; [d] x -1, y, z; [e] - x, - y + 2, - z + 2

The colourless monoclinic crystals of peptide PhCO-Gly-Ala-OCH_2Ph (**2**) are grown from a $CHCl_3$-petroleum ether mixture. The space group is $P2_1$ with one molecule in the asymmetric unit. The solid state structure of peptide **2** is presented in Fig. 5. The molecule adopts an extended conformation characterized by the backbone torsion angles φ_1 = -87.6^o, ψ_1 = -166.5^o at Gly and φ_2 = -154.9^o, ψ_2 = -168.7^o at Ala (Table 2). The self-assembly pattern of peptide **2** is quite similar to that of peptide **1**. The extended structures of the peptide **2** are regularly inter-linked via intermolecular hydrogen bonds between the Gly-NH moiety of one molecule with Ph-CO group of another (N9---O8, 2.86 Å) to create infinite strand-like structure parallel to *a*-axis (Fig. 6a, Table 3). Like peptide **1** these strands are further self-assembled in *c* direction to create two dimensional (*a*, *c* axis) layer of β-sheets (Fig. 6a). Several such layers are stacked in *b* direction through intermolecular hydrogen bond (N13---O12, 2.90 Å) and aromatic π-π

interactions to create laminated supramolecular β-sheet assembly in the solid state (Fig. 6b). The average distance between the eclipsed C atoms of two neighbouring phenyl rings of benzoyl groups is 4.81 Å and that of benzyl groups is also 4.81 Å.

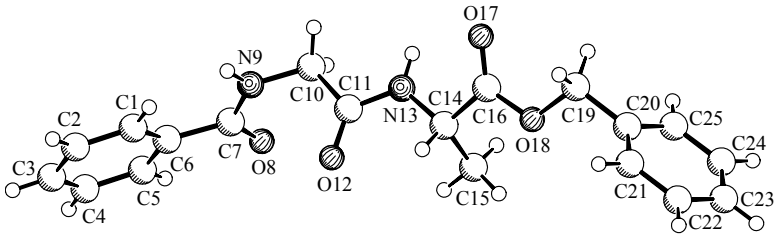

Figure 5. SCHAKAL diagram of peptide **2** with atom numbering scheme.

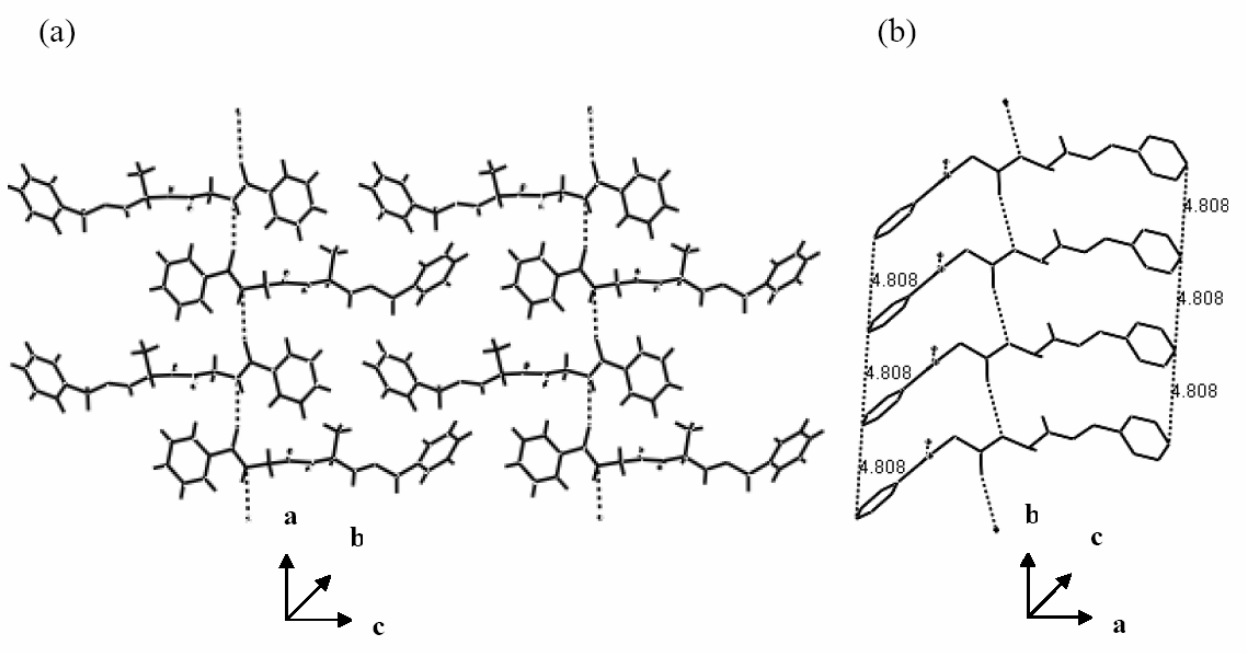

Figure 6. (a) Packing diagram of peptide **2** showing the formation of two dimensional (*a*, *c* axis) layer of β-sheet through intermolecular hydrogen bond (between N9--08) and van der Waals interactions; (b) The molecules of peptide **2** are packed in *b* direction through intermolecular hydrogen bond (between N13---O12) and π-π interactions. Intermolecular hydrogen bonds are shown as dotted lines.

The colourless monoclinic crystals of peptide PhCO-Gly-Aib-OCH_2Ph (**3**) were obtained from ethanol by slow evaporation. The space group is $P2_1/n$ with one molecule in the asymmetric unit. A diagram of peptide **3** is presented in Fig. 7. In contrast to peptide **1** and **2**, peptide **3** adopts a bent structure. The incorporation of helicogenic Aib[14] creates a bent structure where the backbone torsion angles within Gly are φ_1: -168.6° and ψ_1: 179.8° and within Aib they

are φ_2: 54.0° and ψ_2: -155.2° (Table 2). Two neighbouring molecules of peptide **3** are inter-locked by two hydrogen bonds between Aib-NH and Ph-CO (N13---O8, 2.90 Å) to create molecular duplex (Fig. 8a, Table 3). The duplexes are further self-assembled through π-π interactions between the phenyl rings of benzyl groups to create layer (*a*, *c* axis) of β-sheets (Fig. 8b). The distances between the eclipsed C atoms of two neighbouring phenyl rings of benzyl groups are approximately 4.94 Å.

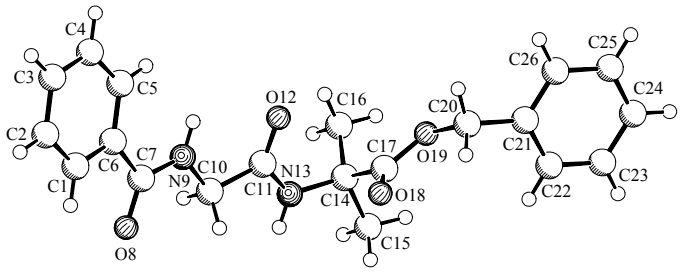

Figure 7. SCHAKAL diagram of peptide **3** with atom numbering scheme.

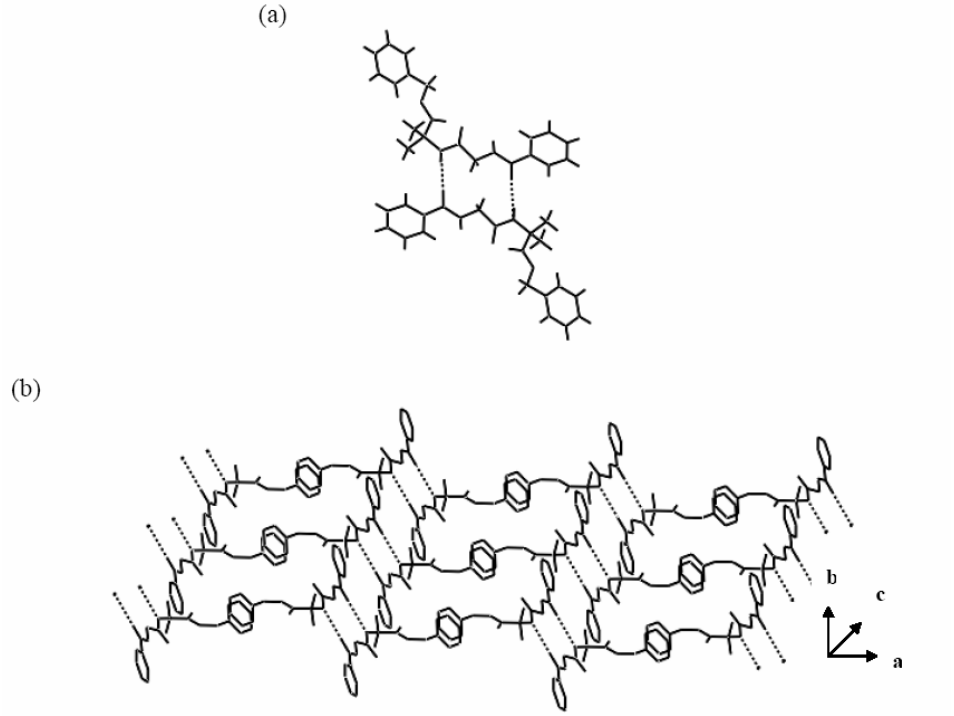

Figure 8. (a) Showing two molecules of peptide **3** are locked by intermolecular hydrogen bonds to create molecular duplex; (b) Packing diagram of peptide **3** showing the formation of two dimensional (*a*, *c* axis) layer of β-sheet through intermolecular hydrogen bonds and π-π interactions between the phenyl rings. Intermolecular hydrogen bonds are shown as dotted lines.

Morphological studies

Recently several reports show that supramolecular β-sheet forming small peptides promote amyloid-like fibrillation in the solid state.[15] Flat laminated ribbon-like materials have been fabricated through β-sheet mediated self-assembly of designed peptide incorporating Pro-Pro segment at the middle.[16] In amyloidogenic peptide calcitonin ribbon-like structures twist back upon themselves to afford hollow tube-like assemblies.[17] Various attempts to fabricate flat ribbon-like structures using amyloid proteins, peptides, and viruses have been reported.[18] It is believed that the quasi-crystalline structures of flat non-twisted morphology may be useful for specific nano-applications.

Therefore, we become interested in exploring the possibility of formation of materials of specific morphology with peptides **1**-**3**. Field emission scanning electron microscopic (FE-SEM) images of the dried fibrous materials of peptides **1**-**3** grown slowly from $CHCl_3$-petroleum ether mixture clearly demonstrate that the aggregates in the solid state are bunches of flat ribbon like structures (Fig. 9). Interestingly peptide **1** generates a net-like structure of ribbons. All peptides exhibit higher ordered self-assembly to create ribbon like materials. The hierarchical assembly of the peptides initially create layers of β-sheets. Subsequently the β-sheet layers stack one on top of the other to produce flat ribbon like structures.

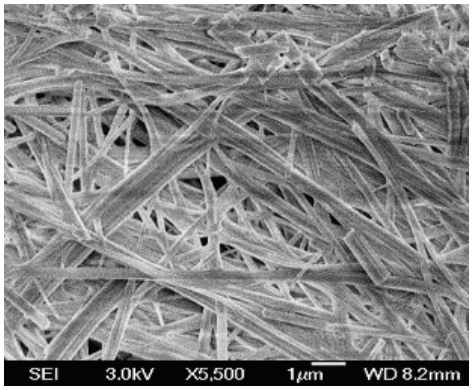

Peptide **1**

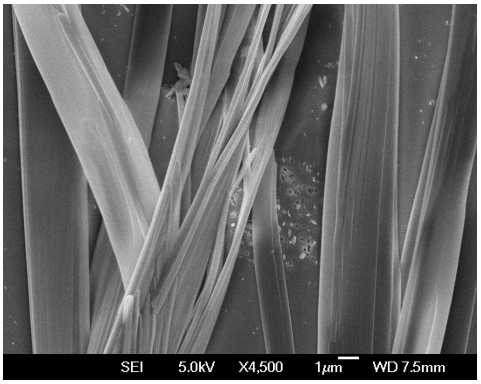

Peptide **2**

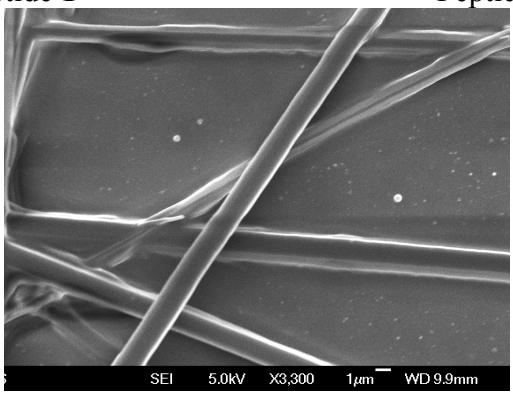

Peptide **3**

Figure 9. The FE-SEM images of the fibrous materials of the peptides showing the formation of flat tape-like morphology. The fibrous materials of the peptides grown slowly from chloroform-petroleum ether are dried and platinum coated for imaging.

Conclusions

The present study shows that the peptides **1-3** can function as subunits in self-assembly. The extended structures of peptide **1** and **2** create layers of β-sheet through zipper-like self-assembly. Subsequently the β-sheet layers are stacked one on top of the other through intermolecular hydrogen bonds and π-π interactions to create supramolecular β-sheet structures. In contrast to peptide **1** and **2** the bent structure of peptide **3** forms molecular duplex, which on self-assembly creates supramolecular β-sheet layers, stabilized by aromatic π-π interactions. Morphological studies show that the peptides **1-3** can generate flat ribbon like materials in the solid state, which are formed through β-sheet mediated self-assembly. The aromatic π-π interactions play a crucial role in the molecular self-assembly and also in the formation of flat ribbon like materials. The investigation establishes that even small dipeptides with aromatic rings at the terminus can generate ribbon like fibrillar structures in the solid state, which may help to understand the structure and function of various abnormal peptides such as prion and the Alzheimer's amyloid.

Experimental Section

Synthesis of peptides

The peptides **1-3** were synthesized by conventional solution phase methods. [19] The benzoyl group was used for N-terminal protection, and the C-terminal was protected as a benzyl ester. Couplings were mediated by dicyclohexylcarbodiimide (DCC). All intermediates were characterized by thin layer chromatography on silica gel and used without further purification. Final peptides were purified by column chromatography using silica gel (100-200 mesh) as the stationary phase and ethyl acetate and petroleum ether mixture as the eluent. The peptides **1-3** were characterized by X-ray crystallography, NMR and IR.

Synthesis of the peptide 1, PhCO-Gly-Gly-OCH_2Ph

PhCO-Gly-OH (2.0 g, 11.2 mmol) was dissolved in DMF (10 ml). Gly-OCH_2Ph obtained from its *p*-toluenesulphonic acid salt (7.5 g, 22.3 mmol) was added to it, followed by DCC (3.45 g, 16.7 mmol). The reaction mixture was stirred at room temperature for 1 day. The precipitated dicyclohexylurea (DCU) was filtered and to the filtrate 20 ml of ethyl acetate was added. The organic layer was washed with 1 N HCl (3 x 30 mL), 1 M Na_2CO_3 solution (3 x 30 mL) and water. The solvent was then dried over anhydrous Na_2SO_4 and evaporated in *vacuo,* giving a white solid. Yield: 3.1 g (85.1 %). Purification was done using silica gel as stationary phase and ethyl acetate-petroleum ether mixture as the eluent. Single crystals were grown from chloroform and petroleum ether mixture (1:3) by slow evaporation and were stable at room temp. Mp = 129-131^{o}C; Anal. Calcd for $C_{18}H_{18}N_2O_4$ (326.35): C, 66.25; H, 5.56; N, 8.58 % ; Found: C, 66.20; H, 5.48; N, 8.50 %; ^{1}H NMR 300 MHz ($CDCl_3$, δ ppm) : 7.84-7.26 (Gly (1) NH, Gly (2) NH, Phenyl ring protons, 12H, *m*), 5.13 (Benzyl protons, 2H, *s*), 4.18 (C^{α}Hs of Gly (2), 2H, *d*, J =

5.4Hz), 4.06 (C^{α}Hs of Gly (1), 2H, *d*, J = 5.4Hz); ^{13}C NMR 75MHz ($CDCl_3$, δ ppm) : 169.76, 169.58, 167.96, 135.07, 133.35, 131.81, 128.56, 128.51, 128.45, 128.23, 127.17, 67.16, 43.53, 41.33; DEPT-135 : 67.16, 43.53, 41.33 (Negative).

Synthesis of the peptide 2, PhCO-Gly-Ala-OCH_2Ph

Peptide **2** was synthesized and purified following the same procedure as that of peptide **1**. Yield: 3.2 g (84.2 %). Single crystals were grown from chloroform and petroleum ether mixture (1:3) by slow evaporation and were stable at room temp. Mp = 126-128^{o}C; Anal. Calcd for $C_{19}H_{20}N_2O_4$ (340.38): C, 67.05; H, 5.92; N, 8.23% ; Found: C, 67.00; H, 5.98; N, 8.17 %; ^{1}H NMR 300 MHz ($CDCl_3$, δ ppm) : 7.82-7.21 (Gly (1) NH, Ala (2) NH, Phenyl ring protons, 12H, m), 5.11 (Benzyl proton, 1H, *d*, J = 12.3), 5.04 (Benzyl proton, 1H, *d*, J = 12.3), 4.56 (C^{α}H of Ala (2), 1H, *m*), 4.16 (C^{α}Hs of Gly (1), 2H, *m*), 1.36 (C^{β}Hs of Ala (2), 3H, *d*, J = 7.2 Hz); ^{13}C NMR 75MHz ($CDCl_3$, δ ppm) : 172.40, 169.15, 167.75, 135.22, 133.28, 131.56, 128.38, 128.30, 128.15, 127.82, 127.10, 66.84, 48.20, 43.39, 17.55; DEPT-135 : 66.84, 43.39 (Negative).

Synthesis of the peptide 3, PhCO-Gly-Aib-OCH_2Ph

Peptide **3** was synthesized and purified following the same procedure as that of peptide **1**. Yield: 3.4 g (85.9 %). Single crystals were grown from ethanol by slow evaporation and were stable at room temp. Mp = 120-122^{o}C; Anal. Calcd for $C_{20}H_{22}N_2O_4$ (354.40): C, 67.78; H, 6.26; N, 7.90 % ; Found: C, 67.70; H, 6.21; N, 7.97 %; ^{1}H NMR 300 MHz ($CDCl_3$, δ ppm) : 7.84-7.25 (Gly (1) NH, Aib (2) NH, Phenyl ring protons, 12H, *m*), 5.15 (Benzyl protons, 2H, *s*), 4.13 (C^{α}Hs of Gly (1), 2H, *d*, J = 5.1Hz), 1.58 (C^{β}Hs of Aib (2), 6H, *s*); ^{13}C NMR 75MHz ($CDCl_3$, δ ppm) : 173.95, 168.31, 167.73, 135.60, 133.49, 131.80, 128.54, 128.46, 128.17, 127.89, 127.13, 67.14, 56.61, 43.79, 24.82; DEPT-135 : 67.14, 43.79 (Negative).

Field emission scanning electron microscopic study

The morphologies of the fibrous materials of peptides **1-3** were investigated using field emission scanning electron microscopy (FE-SEM). For the FE-SEM study, fibrous materials of the peptides (grown slowly from chloroform-petroleum ether) were dried and platinum coated. The micrographs were taken in a FE-SEM apparatus (JEOL JSM-6700F).

X-Ray structure analysis

Data sets were collected with a Nonius KappaCCD diffractometer (Table 4). Programs used: data collection COLLECT, [20] data reduction Denzo-SMN, [21]absorption correction Denzo,[22] structure solution SHELXS-97,[23] structure refinement SHELXL-97,[24] graphics SCHAKAL. [25] CCDC 701759 - 701761 contain the supplementary crystallographic data for this paper. These data can be obtained free of charge at www.ccdc.cam.ac.uk/conts/retrieving.html [or from the Cambridge Crystallographic Data Centre, 12 Union Road, Cambridge CB2 1EZ, UK; fax: (internat.) +44(1223)336-033, E-mail: deposit@ccdc.cam.ac.uk].

Table 4. Crystallographic data for peptides **1-3**

	Peptide **1**	Peptide **2**	Peptide **3**
Formula	$C_{18}H_{18}N_2O_4$	$C_{19}H_{20}N_2O_4$	$C_{20}H_{22}N_2O_4$
Molecular weight	326.34	340.37	354.40
Crystallising solvent	Chloroform &Petroleum ether	Chloroform & Petroleum ether	Ethanol
Crystal colour	Colourless	Colourless	Colourless
Crystal system	Ortho rhombic	Monoclinic	Monoclinic
Space group	*P*bca	$P2_1$	$P2_1/n$
a (Å)	10.0402(3)	4.8076(1)	6.0914(3)
b (Å)	9.0657(2)	9.9798(3)	19.1723(9)
c (Å)	36.4582(13)	18.4813(5)	15.8836(8)
β (^{0})	90.00	96.755(2)	96.115(2)
Z	8	2	4
V (Å^3)	3318.48(17)	880.56(4)	1844.43(16)
Temperature (^{0}C)	-50	-50	-50
μ (cm^{-1})	7.70	7.46	7.32
$D_{calculated}$ (g cm^{-3})	1.306	1.284	1.276
R (int)	0.072	0.040	0.041
No of independent reflections	2960	2715	3245
Reflections with I> 2σ (I)	2170	2519	2646
R_1 (I> 2σ (I))	0.051	0.038	0.051
wR_2 (I> 2σ(I))	0.116	0.090	0.118

Acknowledgements

A.D. and S.K. would like to thank CSIR, New Delhi, India, for providing a senior research fellowship. P.K. thanks UGC, New Delhi for providing Project Fellowship. The financial assistance of UGC, New Delhi is acknowledged [Major Research Project, No.32-190/2006 (SR)].

References and Notes

1. Zhao, X.; Zhang, S. *Chem. Soc. Rev.* **2006**, *35*, 1105.
2. Rajagopal, K.; Schneider, J. P. *Curr. Opin. Struct. Biol.* **2004**, *14*, 480.

3. (a) Holmes, T. C.; Lacalle, S.; Su, X.; Liu, G.; Rich, A.; Zhang. S. *Proc. Natl. Acad. Sci. USA*. **2000**, *97*, 6728. (b) Lashuel, H. A.; LaBrenz, S. R.; Woo, L.; Serpell, L. C.; Kelly, J. W. *J. Am. Chem. Soc.* **2000**, *122*, 5262. (c) Deechongkit, S.; Powers, E. T.; You, S.; Kelly, J. W. *J. Am. Chem. Soc.* **2005**, *127*, 8562.
4. Aggeli, A.; Bell, M.; Boden, N.; Keen, J. N.; Knowles, P. F.; Mcleish, T. C. B.; Pitkeathly, M.; Radford, S. E. *Nature* **1997**, *386*, 259.
5. Kisiday, J. D.; Jin, M.; Kurz, B.; Huang, H.; Semino, C. E.; Zhang, S.; Grodzinsky, A. J. *Proc. Natl. Acad. Sci. U.S.A.* **2002**, *99*, 9996.
6. (a) Taubes, G. *Science* **1996**, *271*, 1493. (b) Lansbury. P. T. *Acc. Chem. Res.* **1996**, *29*, 317. (c) Rochet, J. C.; Lansbury, P. T. *Curr. Opin. Struct. Biol.* **2000**, *10*, 60. (d)Walsh, D. M.; Lomakin, A.; Benedek, G. B.; Condron, M. M.; Teplow, D. B. *J. Biol. Chem.* **1997**, *272*, 22364.
7. (a) Goedert, M.; Spillntini, M. G.; Davies. S. W. *Curr. Opin. Neurobiol.* **1998**, *8*, 619. (b) Baba, M.; Nakajo, S.; Tu, P. H.; Tomita, T.; Nakaya, K.; Lee, V. M. Y.; Trojanowski, J. Q.; Iwatsubo, T. *Am. J. Pathol.* **1998**, *152*, 879. (c) Spillantini, M. G.; Crowther, R. A.; Jakes, R.; Hasegawa, M.; Goedert, M. *Proc. Natl. Acad. Sci. U.S.A.* **1998**, *95*, 6469.
8. (a) Pan, K. M.; Baldwin, M.; Nguyen, J.; Gasset, M.; Serban, A.; Groth, D.; Mehlhorn, I.; Huang, Z.; Fletterick, R. J.; Cohen, F. E. *Proc. Natl. Acad. Sci. U.S.A.* **1993**, *90*, 10962. (b) Prusiner, S. B. *Proc. Natl. Acad. Sci. U.S.A.* **1998**, *95*, 13363.
9. (a) Gillard, R. E.; Raymo, F. M.; Stoddart, J. F. *Chem. -Eur. J.* **1997**, *3*, 1933. (b) Claessens, C. G.; Stoddart, J. F. *J. Phys. Org. Chem.* **1997**, *10*, 254. (c) Shetty, A. S.; Zhang, J.; Moore, J. S. *J. Am. Chem. Soc.* **1996**, *118,* 1019. (d) McGuaghey, G. B.; Gagne, M.; Rappe, A. K. *J. Biol. Chem.* **1998**, *273*, 15458.
10. Gazit, E. *FASEB J.* **2002**, *16*, 77.
11. Reches, M.; Gazit, E. *Amyloid* **2004**, *11*, 81.
12. (a) Toniolo, C.; Palumbo, M. *Biopolymers* **1977**, *16*, 219. (b) Mutter, M.; Maser, F.; Altman, K. H.; Toniolo, C.; Bonora, G. M. *Biopolymers* **1985**, *24*, 1057. (c) Chirgadze, Y. N.; Nevskaya, N. A. *Biopolymers* **1976**, *15*, 627. (d) Baron, M. H.; De Loze, C.; Toniolo, C.; Fasman, G. D. *Biopolymers* 1979, *18*, 411. (e) Moretto, V.; Crisma, M.; Bonora, G. M.; Toniolo, C.; Balaram, H.; Balaram, P. *Macromolecules* **1989**, *22*, 2939.
13. Aravinda, S.; Shamala, N.; Das, C.; Sriranjini, A.; Karle, I. L.; Balaram, P. *J. Am. Chem. Soc.* **2003**, *125*, 5308.
14. Toniolo, C.; Crisma, M.; Formaggio, F.; Peggion, C. *Biopolymers* **2001**, *60*, 396.
15. (a) Naskar, J.; Drew, M. G. B.; Deb, I.; Das, S.; Banerjee, A. *Org. Lett.* **2008**, *10*, 2625. (b) Ray, S.; Das, A. K.; Drew, M. G. B.; Banerjee, A. *Chem. Commun.* **2006**, *40*, 4230. (c) Das, A. K.; Manna, S.; Drew, M. G. B.; Malik, S.; Nandi, A. K.; Banerjee, A. *Supramolecular Chemistry* **2006**, *18*, 645. (d) Ray, S.; Drew, M. G. B.; Das, A. K.; Banerjee, A. *Supramolecular Chemistry* **2006**, *18*, 455. (e) Dutt, A., Drew, M. G. B.; Pramanik, A. *Org. Biomol. Chem.* **2005**, *3*, 2250. (f) Banerjee, A.; Das, A. K.; Drew, M. G. B.; Banerjee, A.

Tetrahedron **2005**, *61*, 5906. (g) Maji, S. K.; Haldar, D.; Banerjee, A.; Banerjee, A. *Tetrahedron* **2002**, *58*, 8695.
16. Lamm, M. S.; Rajagopal, K.; Schneider, J. P.; Pochan, D. J. *J. Am. Chem. Soc.* **2005**, *127*, 16692.
17. Bauer, H. H.; Aebi, U.; Haner, M.; Hermann, R.; Muller, M.; Arvinte, T.; Merkle, H. P. *J. Struct. Biol.* **1995**, *115*, 1.
18. (a) Hartgerink, J. D.; Beniash, E.; Stupp, S. I. *Science* **2001**, *294*, 1684. (b) Sone, E. D.; Stupp, S. I. *J. Am. Chem. Soc.* **2004**, *126*, 12756. (c) Shenton, W.; Douglas, T.; Young, M.; Stubbs, G.; Mann, S. *Adv. Mater.* **1999**, *11*, 253. (d) Scheibel, T.; Parthasarathy, R.; Sawicki, G.; Lin, X. M.; Jaeger, H.; Lindquist, S. L. *Proc. Natl. Acad. Sci. U.S.A.* **2003**, *100*, 4527. (e) Meegan, J. E.; Aggeli, A.; Boden, N.; Brydson, R.; Brown, A. P.; Carrick, L.; Brough, A. R.; Hussain, A.; Ansell, R. *J. Adv. Funct. Mater.* **2004,** *14*, 31. (f) McMillan, R. A.; Paavola, C. D.; Howard, J.; Chan, S. L.; Zaluzec, N. J.; Trent, J. D. *Nat. Mater.* **2002,** *1*, 247. (g) Mao, C.; Flynn, C. E.; Hayhurst, A.; Sweeney, R.; Qi, J.; Georgiou, G.; Iverson, B.; Belcher, A. M. *Proc. Natl. Acad. Sci. U.S.A.* **2003**, *100*, 6946.
19. Bodanszky, M.; Bodanszky, A.; The Practice of Peptide Synthesis; Springer-Verlag: New York, (1984) pp 1-282.
20. Hooft, R. Collect - Data Collection Software, 1998, Nonius B.V., The Netherlands.
21. Otwinowski, Z.; Minor, W. Methods in Enzymology, **1997**, *276*, 307.
22. Otwinowski, Z.; Borek, D.; Majewski, W.; Minor, W. *Acta Cryst.* **2003**, *A59*, 228.
23. Sheldrick, G. M. *Acta Cryst.* **1990**, *A46*, 467.
24. Sheldrick, G. M. *Acta Cryst.* **2008**, *A64*, 112.
25. Keller, E. *SCHAKAL* – A computer program for the graphic representation of molecular and crystallographic models, 1997, University Freiburg, Germany.